Journal of The Electrochemical Society, **156** (7) P101-P106 (2009)
0013-4651/2009/156(7)/P101/6/$25.00 © The Electrochemical Society

Isothermal Oxidation of Ti_2SC in Air

Shahram Amini,[a,z] Andrew R. McGhie,[b] and Michel W. Barsoum[a]

[a]*Department of Materials Science and Engineering, Drexel University, Philadelphia, Pennsylvania 19104, USA*
[b]*Laboratory for Research on the Structure of Matter, University of Pennsylvania, Philadelphia, Pennsylvania 19104, USA*

The oxidation behavior of fully dense Ti_2SC was studied thermogravimetrically in air in the 500–800°C temperature range. The oxidation product was a single-layer of rutile in all cases. At 800°C, the oxide layer was not protective and the oxidation kinetics were rapid. At 600 and 700°C, and up to ~50 h, the kinetics were parabolic before they became linear. It was only at 500°C that the weight gain reached a plateau after a 50 h initial parabolic regime. Mass spectrometry of the gases evolved during oxidation confirmed that both CO_2 and SO_2 are oxidation products. The overall oxidation reaction is thus $Ti_2SC + 4O_2 \rightarrow 2TiO_2 + SO_2 + CO_2$. On the basis of this and previous work, we conclude that oxidation occurs by the outward diffusion of titanium, sulfur, and carbon, the latter two either as atoms or in the form of CO_2 and SO_2 and, most probably, the inward diffusion of oxygen. Mesopores and microcracks were found in all rutile layers formed except those formed at 500°C. The presence of these defects is believed to have led to significantly higher oxidation rates as compared to other rutile-forming ternary carbides, such as Ti_3SiC_2.
© 2009 The Electrochemical Society. [DOI: 10.1149/1.3117348] All rights reserved.

Manuscript submitted December 26, 2008; revised manuscript received March 17, 2009. Published May 6, 2009.

The $M_{n+1}AX_n$ (MAX) phases, where M is an early transition metal, A is an A-group element, and X is C or N) are layered hexagonal solids with two formula units per unit cell, in which near close-packed layers of M are interleaved with layers of a pure group A element, with the X atoms filling the octahedral sites between M layers. It is fairly well established that these phases have an unusual and sometimes unique combination of properties. They are excellent electrical and thermal conductors, thermal shock resistant, and damage tolerant. Despite being elastically quite stiff, they are all readily machinable with nothing more sophisticated than a manual hacksaw.[1-3] Moreover, some of them are fatigue, creep, and oxidation resistant.[4-9]

Titanium sulfur carbide (Ti_2SC) is a member of this class of ternary carbides.[9,10] Like the others, its unit cell is hexagonal (space group D^4_{6h}–$P6_3/mmc$). At 11.22 Å, its c-lattice parameter is the lowest of all MAX phases.[10,11] Because of this low value, partially attributable to the small diameter of S, it was postulated that Ti_2SC could exhibit unusual mechanical properties as compared to the other known MAX phases.[9,11] Elsewhere we have reported on its mechanical, electronic, thermal, magnetic, and elastic properties.[11,12] With an average Vickers hardness of 8 ± 2 GPa in the 2–300 N range, this hardness is the highest of any MAX phase characterized to date. The room-temperature compressive stress was 1.4 ± 0.2 GPa; the failure mode was brittle. Its Young's modulus, also one of the highest for a M_2AX phase measured to date, was 316 ± 2 GPa. Unlike all other MAX phases known to date, wherein their loading–unloading stress–strain curves outline nonlinear, fully reversible, strain-rate–independent, reproducible, closed hysteretic loops, there was no evidence for the formation of incipient kink bands during simple compression and the behavior was nearly fully elastic until failure.[11] The room-temperature thermal conductivity (≈60 W/mK) is also one of the highest of any MAX phase measured to date.

The Young's, shear, and bulk moduli, determined from ultrasonic measurements, are 290, 125, and 145 GPa, respectively.[12] Its electrical conductivity is metallic-like and equal to $1.9 \times 10^6\ \Omega^{-1}\ m^{-1}$ at room temperature. The Debye temperature is 765 K.[12] The bulk modulus, calculated using the Birch–Murnaghan equation of state, is 191 ± 3 GPa,[13] which is comparable to those of Ti_2AlC, Nb_2AlC, and V_2AlC. In another recent paper, we have shown that the tribological properties of Ti_2SC against alumina are excellent over the 25–550°C range.[14]

Elsewhere, we reported on the thermal expansion and stability of Ti_2SC powders in air and Ar atmospheres using high-temperature X-ray diffraction.[15] Ti_2SC is stable in Ar atmosphere up to ≈400°C; above this temperature, it dissociates into TiS_2. With little anisotropy in thermal expansion, its volumetric thermal expansion was calculated to be $(25.2 \times 10^{-6})°C^{-1}$. In air, at 400°C, the powders start to oxidize into anatase, which, in turn, transforms into rutile at higher temperatures. This recent work was qualitative and was carried out on powders.

In this report on the oxidation of bulk samples, it is useful to briefly review the oxidation kinetics and morphology of the oxide phases that form after long-term oxidation of other Ti-containing MAX phases in air. When polycrystalline samples of Ti_3SiC_2, Ti_3SiC_2–30 vol % TiC, and Ti_3SiC_2–30 vol % SiC are oxidized in air in the 900–1400°C range, the scales that formed were dense, adherent, and resistant to thermal cycling. The oxidation mostly resulted in a duplex oxide layer (an inner TiO_2/SiO_2 layer and an outer rutile layer); the kinetics are initially parabolic, but become linear at longer times.[16-18]

The oxidation of $Ti_{n+1}AlC_n$ ternaries in the 800–1100°C range resulted in a rutile layer in which some Al is dissolved.[19] It has also been shown that subtle changes in chemistry can result in the formation of pure Al_2O_3 layers. For example, Sundberg et al.[20] have shown that Ti_2AlC forms an excellent Al_2O_3 layer that is exceedingly protective, even under intense thermal cycling. Wang and Zhou also reported the formation of dense protective alumina layers on the surfaces of Ti_3AlC_2 and Ti_2AlC, in Ref. 21 and 22, respectively, when oxidized in air. When the Ti_2AlC and $Ti_2AlC_{0.5}N_{0.5}$ solid solution are oxidized in air, the oxidation products are comprised of a duplex oxide layer of rutile-based solid solution and Al_2O_3. In the 1000–1100°C temperature range and for short times (≈20 h), the oxidation kinetics are parabolic. At 900°C, the kinetics are quasi-linear, and up to 100 h, the outermost layers that form are almost pure rutile, dense, and protective.[19] In $Ti_4AlN_{2.9}$ and Ti_3AlC_2, at short times (<10 h), the oxidation kinetics are parabolic in the 800–1100°C temperature range but become linear at longer times. The scales that form are comprised mainly of a rutile-based solid solution and some Al_2O_3.[19]

In Ti_3GeC_2 and $Ti_3(Ge_{0.5}Si_{0.5})C_2$, at 800°C and higher, the oxide layers formed are not protective and the oxidation kinetics are linear. At higher temperatures, GeO_2 whiskers, visible to naked eye, form on the surface of the Ti_3GeC_2.[23]

Herein, we report on the isothermal oxidation behavior of bulk Ti_2SC samples in air in the 500–800°C temperature range. From a technological point of view, it is crucial to determine whether the oxidation kinetics remain parabolic or become linear. More importantly, given that the oxidation products of both C and S are gases, it was postulated that its oxidation behavior may be considerably different from other Ti-containing MAX phases.

[z] E-mail: shahram@drexel.edu

Downloaded 21 Dec 2010 to 130.91.117.41. Redistribution subject to ECS license or copyright; see http://www.ecsdl.org/terms_use.jsp

Experimental

Phase-pure 325 mesh Ti_2SC powders (3-ONE-2, Voorhees, NJ) were hot-pressed in a graphite-heated, vacuum atmosphere hot press (Series 3600, Centorr Vacuum Industries, Somerville, MA). The powder was poured and wrapped in graphite foil, which, in turn, was placed in a graphite die and heated at 10°C/min and was held for ~5 h, at 1500°C. A load, corresponding to a stress of ~45 MPa, was applied at 500°C and maintained throughout the entire process. More details are reported in Ref. 11.

The oxidation study was carried out using a D-101 CAHN thermobalance (Thermo Electron Co., Waltham, MA). The resolution of our balance was 0.1 mg. Rectangular specimens ($4 \times 4 \times 10$ mm) were machined out of the bulk samples using a precision diamond blade. All sides of the samples were polished down to 1200 grit SiC paper. The samples were placed in an alumina crucible that was hung by a platinum wire to the balance. The samples were oxidized in air at 500, 600, 700, and 800°C for various times that ranged from 50 to 300 h.

At 700°C after 300 h, the experiment was followed by cyclic oxidation where the sample was cooled in the furnace to room temperature and heated up again to 700°C six consecutive times. The signal collected from the thermobalance was smoothed by signal averaging over the entire run in order to reduce the noise. The latter was done by KalidaGraph software, in which a Stineman function was applied.

For calibration purposes, five small $4 \times 4 \times 4$ mm electron-discharged-machined cubes were oxidized in a box furnace in air at 500, 600, and 700°C for 300 h. Samples' weights were measured by a HR-202i Analytical Balance (A&D Weighing, San Jose, CA) with a resolution of 0.01 mg, before and after oxidation. These results were used to calibrate the thermobalance data for accuracy when needed because the noise level in the latter was sometimes high.

We also carried out a thermogravimetric thermal analysis (TGA) measurement in air on bulk samples in a simultaneous TGA–differential thermal analysis (DTA) unit (2960 SDT, TA Instruments, New Castle, DE) with a highly precise, horizontal dual balance, in which the exhaust gas port was connected to a mass spectrometer (Benchtop Thermostar, Pfeiffer Vacuum Inc., Nashua, NH) for analysis of the gases evolved during the experiment. The heating rate in this experiment was 20°C/min.

X-ray diffraction (XRD) patterns of the oxidized surface were obtained using a diffractometer (model 500D, Siemens, Karlsruhe, Germany). The spectra were collected at a step scan of 0.02 2θ and a step time of 1 s.

The microstructure of the samples was observed using a field-emission scanning electron microscope [(SEM), Zeiss Supra 50VP, Germany] after cross-sectioning, mounting, and polishing the oxidized samples with diamond solutions down to 1 μm.

Results and Discussion

Figure 1 shows the XRD patterns of the oxide scales formed at 500 and 800°C. The patterns at 600 and 700°C are similar to those at 800°C and are not shown. A single rutile layer was found to be the reaction product at all temperatures. This is not too surprising, given that the oxidation products of both C and S are gases (further details follow) and consistent with the results on Ti_2SC powders.[15] Note that Ti_2SC peaks exist only at 500°C, because at 2–3 μm, the rutile layer formed is quite thin.

Figure 2 shows the weight gain due to oxygen uptake in the TGA/mass spectrometer. These results unambiguously show that the weight gain starts at ≈600°C; SO_2 and CO_2 are evolved at ≈900°C. We take the lag between the temperature at which oxidation commences and the time SO_2 and CO_2 are evolved to indicate that the latter only start evolving after the oxide layer thickness reaches a critical value and/or the pressure of the gases is high enough to cause fissures, pores, and/or microcracks. Such a conjecture is also consistent with the fact that the kinetics start off parabolic, but then become linear after longer times (further details follow).

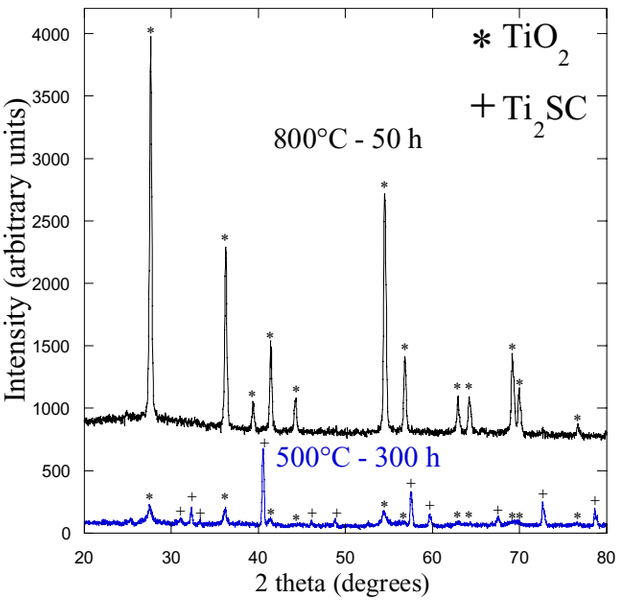

Figure 1. (Color online) XRD patterns of bulk Ti_2SC samples oxidized in air at 500 and 800°C for 300 and 50 h, respectively. In all cases, rutile is the oxidation product phase. Because at 500°C, the rutile layer formed is quite thin, peaks belonging to Ti_2SC are observed.

On the basis of these and the XRD results, there is little doubt that the oxidation reaction of Ti_2SC in air is given by

$$Ti_2SC + 4O_2 \rightarrow 2TiO_2 + SO_2 + CO_2 \quad [1]$$

Clearly the S and C diffuse out; whether the diffusion is atomic and/or in the form of SO_2 and CO_2 is unknown at this time. Similarly, whether the Ti diffuses out or the oxygen diffuses in is also unclear, but based on our previous work, it is reasonable to assume that both diffuse.[17] These comments notwithstanding, it is hereby acknowledged that more work is needed to better delineate the sequence of events that result in gas evolution.

The time dependency of the weight gain, Δw, that occurs during the oxidation of Ti_2SC in air is shown in Fig. 3a, based on which it

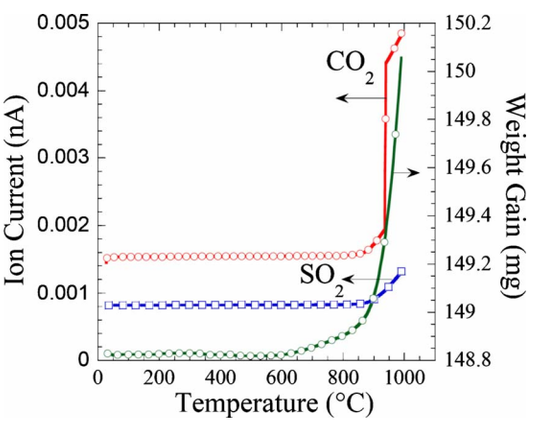

Figure 2. (Color online) Temperature dependencies of weight gain (right axis) and composition (left axis) of gases evolved during simultaneous TGA/DTA oxidation of bulk Ti_2SC samples heated at 20°C/min in air. At ~900°C, a clear signal for the evolution of CO_2 and SO_2 was obtained.

Downloaded 21 Dec 2010 to 130.91.117.41. Redistribution subject to ECS license or copyright; see http://www.ecsdl.org/terms_use.jsp

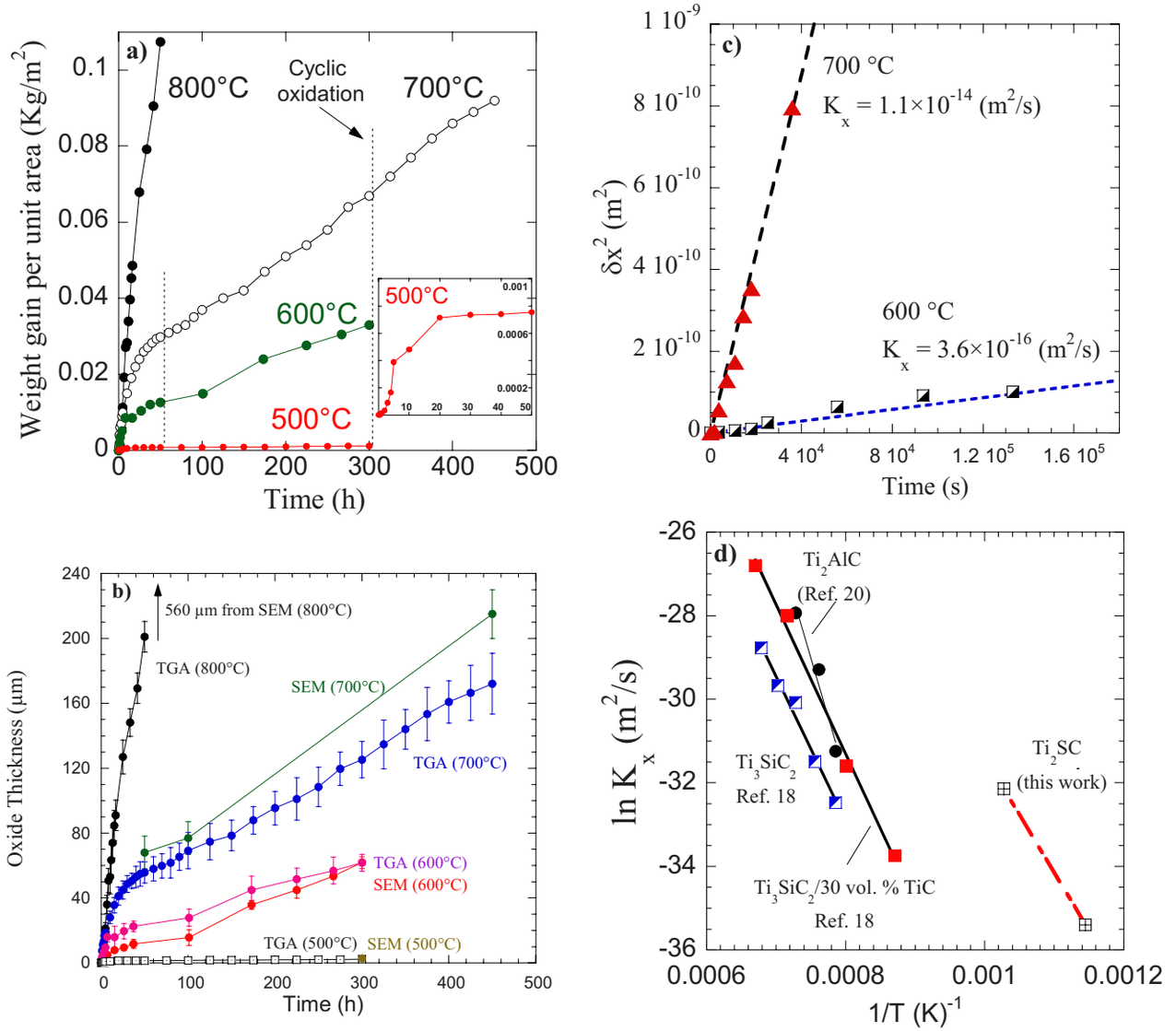

Figure 3. (Color online) (a) Weight gain, normalized by surface area, as a function of time and temperature for Ti_2SC. At 700°C after 300 h, the sample was cycled six times for a total of ≈450 h. Inset shows weight gain at 500°C for the first 50 h only. (b) Comparison of oxide thickness, Δx, calculated from the weight gains assuming Reaction 1 and those measured directly in the SEM. (c) Plot of Δx^2 vs time for first 50 h of oxidation at 600 and 700°C; the 700°C data were determined from the results shown in (b) (see the Appendix); (d) Arrhenius plot of K_x. Also shown are the results for Ti_2AlC,[19] Ti_3SiC_2, Ti_3SiC_2–30 vol % TiC, and Ti_3SiC_2–30 vol % SiC.[17]

is clear that at 800°C the oxidation rate is quite high, (i.e., catastrophic). At 600 and 700°C, the oxidation kinetics are initially parabolic up to ~50 h; at $t >$ ~ 50 h, the oxidation kinetics become linear. It is only at 500°C that, after an initial parabolic regime up to ~50 h (inset of Fig. 3a), the weight gain appears to saturate. Clearly, these results will limit the use of Ti_2SC components in air to temperatures not much higher than 500°C.

The Δw that occurs during the oxidation was converted to an oxide thickness Δx (see Appendix), and the results are plotted in Fig. 3b, together with the oxide thicknesses measured directly in the SEM. The weight gain associated with Reaction 1 is ≈21%, and thus, to convert the Δw results shown in Fig. 3a to Δx, the former is multiplied by 1.87×10^{-3} (Appendix). Possible reasons for the discrepancies observed in Fig. 3b between the SEM results and those obtained by converting Δw to Δx at 600, 700, and 800°C are discussed below.

To try and explore the nature of the rate-limiting step during early oxidation of Ti_2SC, the time dependencies, up to only 50 h, of Δx^2 of the oxide layer at 600 and 700°C are plotted in Fig. 3c. The linear relationship, obvious in Fig. 3c, implies that

$$\Delta x^2 = 2K_x t \qquad [2]$$

where K_x (m^2/s), is the parabolic rate constant.[24] From these results, K_x at 600 and 700°C are calculated to be 3.6×10^{-16} and 1.1×10^{-14} m^2/s, respectively. When these two data points are plotted on an Arrhenius plot (Fig. 3d), it is clear that the parabolic rate constant for Ti_2SC is roughly an order of magnitude faster than that reported in previous works.[15,17,19,25] The reasons for this state of affairs could be related to either the fact that the layers, even at short times, are not fully dense (further details follow) and/or aliovalent impurities, such as Fe present in the initial powders (long collection time energy dispersive spectroscopy indicated ~2 wt % Fe[13]), create vacancies on the oxygen or titanium sublattices, thereby enhancing the rate-limiting step, which is believed to be ionic diffusion in

Downloaded 21 Dec 2010 to 130.91.117.41. Redistribution subject to ECS license or copyright; see http://www.ecsdl.org/terms_use.jsp

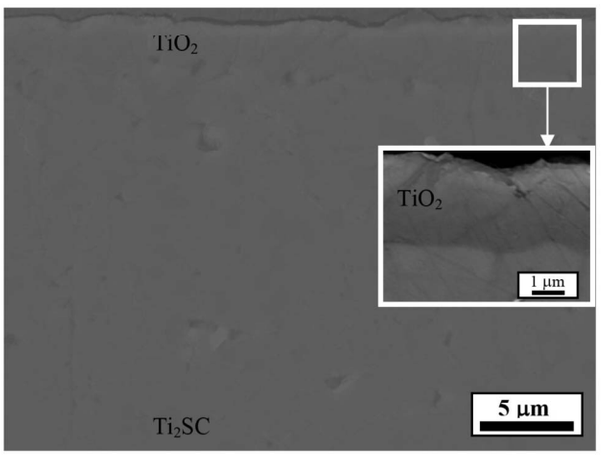

Figure 4. Secondary electron SEM image of the oxide layer formed at 500°C after 300 h in air. Inset shows a backscattered SEM image of the same sample.

the rutile layer.[17,19,25] The fact that the activation energy for the two data points obtained here is nearly identical to that of previous work[17] strongly suggests the latter explanation. This conclusion is similar to and consistent with the fact that the initial oxidation kinetics of the $Ti_{n+1}AlC_n$ compounds are faster than those of Ti_3SiC_2 due to the presumed formation of oxygen vacancies when Al ions are dissolved in the rutile layer.[19,25]

Figure 4 shows a typical secondary electron SEM image of the oxide layer formed on the surface after oxidation at 500°C for 300 h. The inset shows a backscattered electron SEM image of the same sample, clearly showing a contrast between the rutile layer and the underlying substrate. Figures 5-7 show typical secondary electron SEM images of the oxide layers formed on the surface at 600, 700, and 800°C, for various times, respectively. From these SEM images, the following is obvious:

1. At 500°C, the oxide layer (Fig. 4) did not flake off, but remained adherent, dense, apparently crack free, and protective, and was significantly thinner than the oxide layers formed at the higher temperatures explored herein.

2. The oxide layers formed on the surface after oxidation at 600°C for 300 h (Fig. 5a) and at 700°C for 450 h (Fig. 6a) did not flake off either and remained adherent to the Ti_2SC substrate. At higher magnifications, however, the SEM images show the presence of mesopores and microcracks throughout the oxide layers formed at 600°C (Fig. 5b and c) and 700°C (Fig. 6b-d). Note that after 300 h oxidation at 700°C, the sample was cycled six times from room temperature to 700°C.

3. The oxide layer formed after oxidation at 800°C for 50 h (Fig. 7a) is quite thick and did not adhere to the substrate. Here again, at higher magnifications, mesopores and microcracks (Fig. 7b-d) were present throughout the oxide layer, but at a volume fraction that was significantly higher than samples oxidized at 700 and 600°C. If the rate of oxidation of the S and C atoms is faster than their diffusion outward, a gas pressure will build up in the rutile. It is reasonable to assume that this pressure can in turn result in the microcracks and fissures observed.

With this information, the reasons for the discrepancies alluded to earlier become more transparent. The oxide layers formed at 600, 700, and 800°C, after an initial 50 h period, are not fully dense, which would explain the change in kinetics from parabolic to linear. At 800°C, the volume fraction of cracks and pores are sufficiently high that the scale appears thicker than it should be based on the weight gain.

Conclusions

The oxidation product of bulk Ti_2SC samples at all temperatures tested is a single rutile scale, SO_2 and CO_2. The oxidation reaction is thus: $Ti_2SC + 4O_2 \rightarrow 2TiO_2 + SO_2 + CO_2$. At 800°C, the oxide layer was thick, non-adherent, and not protective, resulting in catastrophic oxidation. At lower temperatures, the oxide scales were adherent and, at least at 700°C, resistant to spalling after six heating and cooling cycles. At 600 and 700°C and up to ~50 h, the kinetics were initially parabolic, before becoming linear. The reason for the

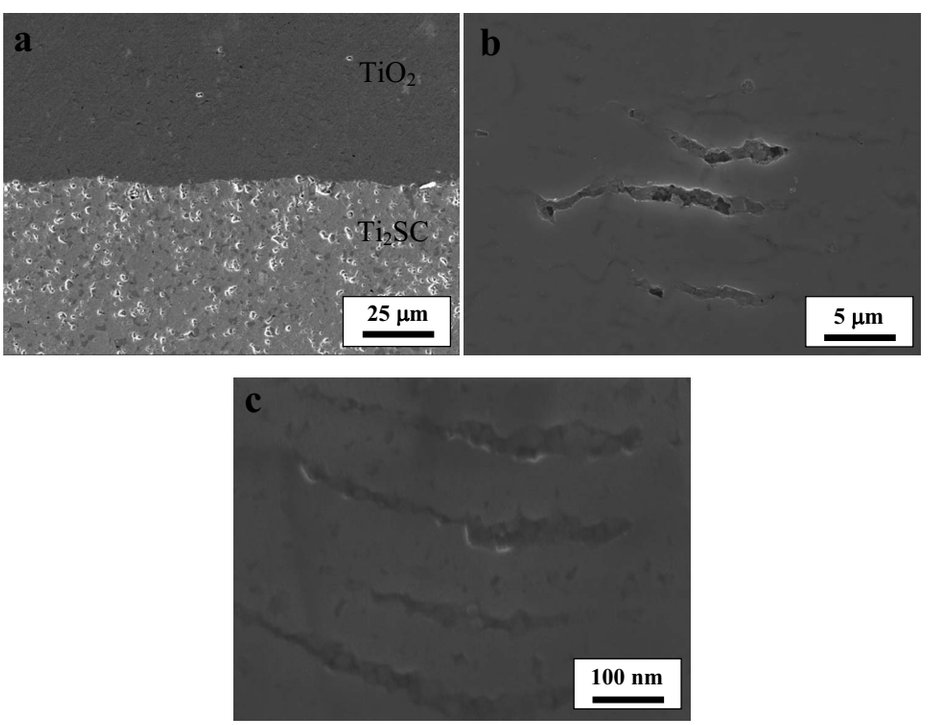

Figure 5. SEM images of oxide layers formed at 600°C after 300 h in air: (a) at low magnification and (b,c) at higher magnifications showing the presence of mesopores and microcracks.

Downloaded 21 Dec 2010 to 130.91.117.41. Redistribution subject to ECS license or copyright; see http://www.ecsdl.org/terms_use.jsp

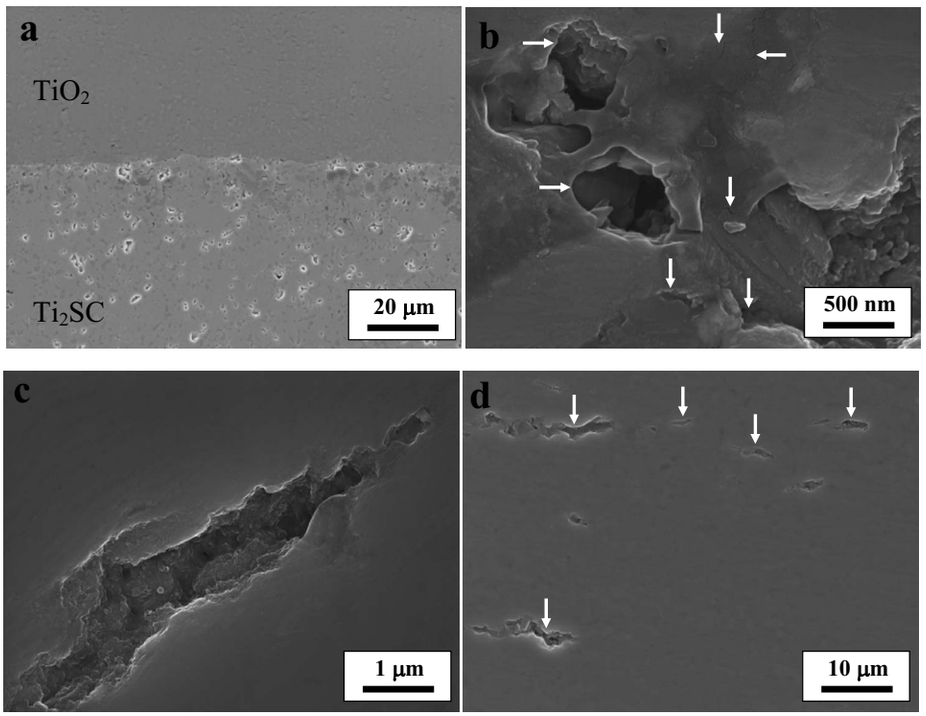

Figure 6. SEM images of oxide layers formed at 700°C after 450 h in air: (a) at low magnification and (b, c, and d) at higher magnifications showing the presence of mesopores and microcracks shown by arrows.

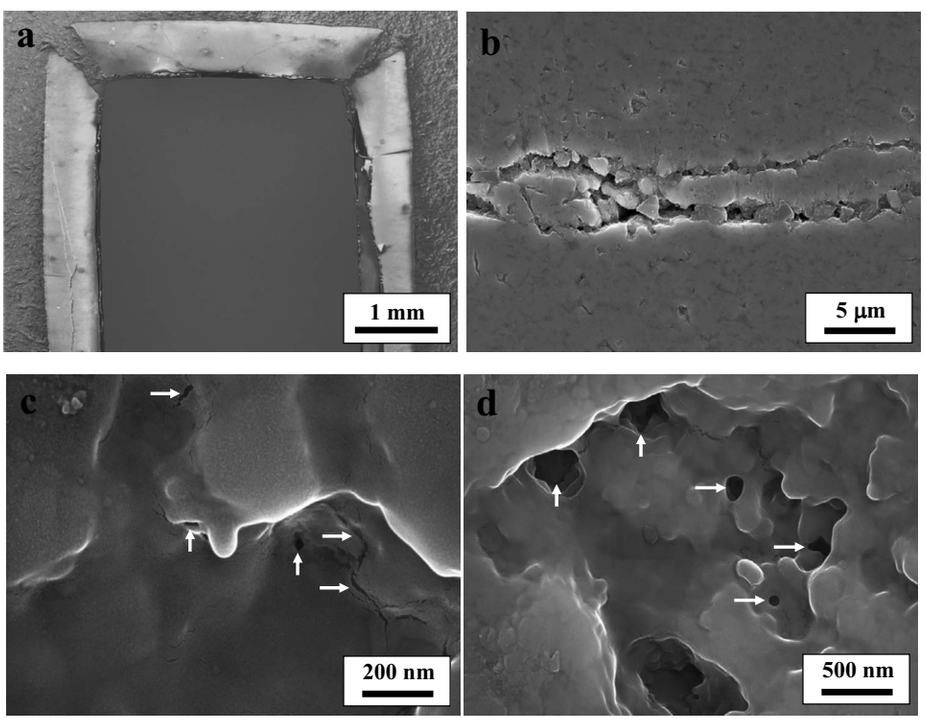

Figure 7. SEM images of oxide layers formed at 800°C after 50 h in air: (a) at low magnification and (b, c, and d) at higher magnifications showing the presence of mesopores and microcracks shown by arrows. Note that volume fraction of the latter is significantly greater than those formed at lower temperatures.

transition is believed to be the formation of pores and microcracks in the rutile layer at longer times. It is only at 500°C that the weight gain reaches a plateau at longer soaking times ($t > 50$ h). It follows that the maximum use temperature for Ti_2SC in air will be in the vicinity of 500°C. On the basis of the results of this work, we conclude that the oxidation occurs by the outward diffusion of C and S either as atoms or in the form of CO_2 and SO_2. At this point, it is not clear whether the Ti diffuses out or the O diffuses in. On the basis of pervious works, however, it is reasonable to assume both ions are counterdiffusing.

Acknowledgment

This work is funded by NSF grant no. DMR-0736218 and no. DMR-050371.

Downloaded 21 Dec 2010 to 130.91.117.41. Redistribution subject to ECS license or copyright; see http://www.ecsdl.org/terms_use.jsp

Drexel University assisted in meeting the publication costs of this article.

Appendix

The oxidation of one mole of Ti_2SC results in two moles of rutile (Eq. 1), which translates to a weight gain of 0.02 kg/mole of Ti_2SC. The molar volume of fully dense rutile is assumed to be 18.7 cm^3/mole. The thickness of two moles of rutile formed when extended over 1 m^2 is $2 \times 18.7 \times 10^{-6} = 3.74 \times 10^{-5}$ m. It follows that when converting weight gains per meter squared to oxide thickness in meters, the former is to be multiplied by $3.74 \times 10^{-5}/0.02 = 1.87 \times 10^{-3}$ m/kg/m^2.

References

1. M. W. Barsoum and T. El-Raghy, *J. Am. Ceram. Soc.*, **79**, 1953 (1996).
2. M. W. Barsoum, D. Brodkin, and T. El-Raghy, *Scr. Mater.*, **36**, 535 (1997).
3. M. W. Barsoum and M. Radovic, in *Encyclopedia of Materials Science and Technology*, K. H. J. Buschow RWC, M. C. Flemings, E. J. Kramer, S. Mahajan, and P. Veyssiere, Editors, Elsevier, Amsterdam (2004).
4. M. W. Barsoum, T. El-Raghy, C. J. Rawn, W. D. Porter, H. Wang, A. Payzant, and C. Hubbard, *J. Phys. Chem. Solids*, **60**, 429 (1999).
5. I. M. Low, S. K. Lee, B. Lawn, and M. W. Barsoum, *J. Am. Ceram. Soc.*, **81**, 225 (1998).
6. M. W. Barsoum and T. El-Raghy, *Metall. Mater. Trans. A*, **30A**, 363 (1999).
7. M. W. Barsoum and T. El-Raghy, *J. Mater. Synth. Process.*, **5**, 197 (1997).
8. T. El-Raghy, M. W. Barsoum, A. Zavaliangos, and S. R. Kalidindi, *J. Am. Ceram. Soc.*, **82**, 2855 (1999).
9. M. W. Barsoum, *Prog. Solid State Chem.*, **28**, 201 (2000).
10. H. Nowotny, *Prog. Solid State Chem.*, **2**, 27 (1970).
11. S. Amini, M. W. Barsoum, and T. El-Raghy, *J. Am. Ceram. Soc.*, **90**, 3953 (2007).
12. T. H. Scabarozi, S. Amini, P. Finkel, O. D. Leaffer, J. E. Spanier, M. W. Barsoum, M. Drulis, H. Drulis, W. M. Tambussi, J. D. Hettinger, et al., *J. Appl. Phys.*, **104**, 033502 (2008).
13. S. R. Kulkarni, R. S. Vennila, N. A. Phatak, S. K. Saxena, C. S. Zha, T. El-Raghy, M. W. Barsoum, W. Luo, and R. Ahuja, *J. Alloys Compd.*, **448**, L1 (2008).
14. S. Gupta, S. Amini, D. Filimonov, T. Palanisamy, T. El-Raghy, and M. W. Barsoum, *J. Am. Ceram. Soc.*, **90**, 3566 (2007).
15. S. R. Kulkarni, M. Merlini, N. Phatak, S. K. Saxena, G. Artioli, S. Amini, and M. W. Barsoum, *J. Alloys Compd.*, **469**, 395 (2009).
16. M. W. Barsoum, T. El-Raghy, and L. Ogbuji, *J. Electrochem. Soc.*, **144**, 2508 (1997).
17. M. W. Barsoum, L. H. Ho-Duc, M. Radovic, and T. El-Raghy, *J. Electrochem. Soc.*, **150**, B166 (2003).
18. R. Radhakrishnan, J. J. Williams, and M. Akinc, *J. Alloys Compd.*, **285**, 85 (1999).
19. M. W. Barsoum, N. Tzenov, A. Procopio, T. El-Raghy, and M. Ali, *J. Electrochem. Soc.*, **148**, C551 (2001).
20. M. Sundberg, G. Malmqvist, A. Magnusson, and T. El-Raghy, *Ceram. Int.*, **30**, 1899 (2004).
21. X. H. Wang and Y. C. Zhou, *Corros. Sci.*, **45**, 891 (2003).
22. X. H. Wang and Y. C. Zhou, *Oxid. Met.*, **59**, 303 (2003).
23. S. Gupta, A. Ganguly, D. Filimonov, and M. W. Barsoum, *J. Electrochem. Soc.*, **153**, J61 (2006).
24. M. W. Barsoum, *Fundamentals of Ceramics*, Institute of Physics, Bristol (2003).
25. M. W. Barsoum, *J. Electrochem. Soc.*, **148**, C544 (2001).

Downloaded 21 Dec 2010 to 130.91.117.41. Redistribution subject to ECS license or copyright; see http://www.ecsdl.org/terms_use.jsp